Nature of the Band Gap and Origin of the Conductivity of PbO_2 Revealed by Theory and Experiment

David O. Scanlon, Aoife B. Kehoe, and Graeme W. Watson
School of Chemistry and CRANN, Trinity College Dublin, Dublin 2, Ireland

Martin O. Jones and William I. F. David
ISIS Facility, Rutherford Appleton Laboratory, Chilton, Didcot, Oxon OX11 0QX, UK Department of Chemistry, Chemistry Research Laboratory, University of Oxford, Mansfield Road, Oxford OX1 3TA, United Kingdom

David J. Payne, Russell G. Egdell, and Peter P. Edwards
Department of Chemistry, Chemistry Research Laboratory, University of Oxford, Mansfield Road, Oxford OX1 3TA, United Kingdom

Aron Walsh
Centre for Sustainable Chemical Technologies and Department of Chemistry, University of Bath, Claverton Down, Bath BA2 7AY, United Kingdom
(Received 6 October 2011; published 7 December 2011)

Lead dioxide has been used for over a century in the lead-acid battery. Many fundamental questions concerning PbO_2 remain unanswered, principally: (i) is the bulk material a metal or a semiconductor, and (ii) what is the source of the high levels of conductivity? We calculate the electronic structure and defect physics of PbO_2, using a hybrid density functional, and show that it is an *n*-type semiconductor with a small indirect band gap of $\sim$0.2 eV. The origin of electron carriers in the undoped material is found to be oxygen vacancies, which forms a donor state resonant in the conduction band. A dipole-forbidden band gap combined with a large carrier induced Moss-Burstein shift results in a large effective optical band gap. The model is supported by neutron diffraction, which reveals that the oxygen sublattice is only 98.4% occupied, thus confirming oxygen substoichiometry as the electron source.

DOI: 10.1103/PhysRevLett.107.246402 PACS numbers: 71.20.−b, 61.72.S−, 82.47.Cb

Since the invention of the lead-acid battery in 1860, [1] lead dioxide has been of great practical importance due to its utility in many electrochemical processes. [2] These applications depend strongly on the electrical conductivity and redox chemistry of the material [2,3]. While high levels of conductivity are well established, the electronic structure of PbO_2 has been a source of controversy in the literature, and to date remains uncertain. It has been postulated that PbO_2 is intrinsically metallic [4–9], but conversely, the carrier concentrations have been reported to vary strongly with oxygen partial pressure [10], indicating a mechanism of lattice defect controlled conductivity. Whereas previous band structure calculations based on density functional theory (DFT) found that the conduction band of PbO_2 overlaps with the top of the valence band (semimetallic) [7,11], optical band gaps have been reported in the literature of the order of 1.4–2.9 eV [12,13]. It is clear that there is a pressing need for a careful reexamination of the physical properties of PbO_2.

In addition to the electronic structure, the role of lattice defects in PbO_2 has also been a cause for much debate [14,15]. PbO_2 typically displays degenerate *n*-type conductivity, with undoped samples possessing carrier concentrations of $\sim 10^{19}$–10^{21} cm^{-3} [7,10], depending on sample preparation conditions. This conductivity has been attributed to oxygen vacancies (V_O) [16], lead interstitials (Pb_i) [17], and adventitious incorporation of hydrogen into the system [12,15,18].

In the lead-acid battery, it has been reported that PbO_2 electrodes are substoichiometric on the *cation* sublattice, and not on the anion sublattice, based on neutron diffraction experiments [14,15,19]. Even recent studies refer to the fact that the oxygen sublattice is ''complete'' [2]. The presence of lead vacancies (V_{Pb}) as the dominant defect species should cause a considerable number of hole carriers in the system, although *p*-type PbO_2 has never been reported. In isostructural and isoelectronic SnO_2, the formation energy of a cation vacancy is much higher than that of the anion vacancy [20,21], and a similar behavior would be expected here.

In this Letter, through a combination of first-principles band structure calculations and experimental characterization of PbO_2, we present the first consistent explanation for the material behavior. PbO_2 has a small but finite band gap and a light electron effective mass. The calculated charge neutrality level lies deep in the conduction band, which is consistent with high levels of electrical conductivity. Conduction electrons are created through oxygen loss,

which is an exothermic process in the noninteracting limit, as confirmed by neutron diffraction measurements.

Computational Method.—All DFT calculations were performed using the VASP code [22]. Interactions between the core and valence electrons described within the scalar-relativistic projector augmented-wave (method) [23]. The calculations were performed using the Perdew-Burke-Ernzerhof (PBE) [24] exchange-correlation functional augmented with 25% screened Hartree-Fock exchange, producing the Heyd-Scuseria-Ernzerhof (HSE06) functional [25]. HSE06 has been successful in reproducing the structural and band gap data for a wide range of metal oxide systems [26–35]. Plane wave cutoff and k-point sampling were tested, with a cutoff of 400 eV and a k-point sampling of $6 \times 6 \times 4$ for the 6 atom unit cell of PbO_2 found to be sufficient. The ionic forces were converged to less than 0.01 eV Å^{-1}. The optical transition matrix elements, calculated following Fermi's golden rule, were used to construct the imaginary dielectric function and the corresponding optical absorption spectrum [36]. Point defects were calculated in their various charge states in a $2 \times 2 \times 3$ (72 atom) supercell with a $2 \times 2 \times 2$ Monkhorst-Pack k-point grid, and all calculations were spin polarized (e.g., the singly charged O vacancy defect was treated as a spin doublet).

The formation energy of a defect with charge state q is given by

$$\Delta H_f(D, q) = (E^{(D,q)} - E^{\mathrm{H}}) + \sum_i n_i(E_i + \mu_i) + q(E_{\mathrm{Fermi}} + \epsilon^{\mathrm{H}}_{\mathrm{VBM}}) + E_{\mathrm{align}}[q], \quad (1)$$

where E^{H} is the total energy of the host supercell and $E^{(D,q)}$ is the total energy of the defect-containing cell [37,38]. Elemental reference energies, E_i, were obtained from the calculated standard states and n is the number of atoms formally added to or taken away from an external reservoir. The chemical potentials, μ_i, reflect the equilibrium growth conditions, within the global constraint of the calculated enthalpy of the host, in this instance PbO_2: $\mu_{\mathrm{Pb}} + 2\mu_{\mathrm{O}} = \Delta H_f^{\mathrm{PbO_2}} = -2.56$ eV. E_{Fermi} represents the electron chemical potential, which ranges from the valence to conduction band edges. $\epsilon^{\mathrm{H}}_{\mathrm{VBM}}$ is the eigenvalue of the valence band maximum (VBM) of the bulk material. $E_{\mathrm{align}}[q]$ accounts for: (i) the proper alignment of the electrostatic potential between the bulk and the defective supercells and (ii) corrections for the finite-size effects in the calculation of charged impurities, as outlined by Freysoldt *et al.* [39], using an isotropic dielectric constant $\epsilon_0 = 10$. Band filling by resonant defect levels was treated using the standard approach [40]. The chemical potential limit of the O-poor conditions was checked, with PbO found to be a competitive phase.

Experimental Method.—Powder neutron diffraction was performed on a 5 g sample of commercially available PbO_2 powder (Sigma Aldrich, U.K., 99.999% pure) at the ISIS Spallation Neutron Source facility, Rutherford Appleton Laboratory, U.K. Samples were held in vanadium cans and all data collected on the Polaris diffractometer [41]. The diffraction data were fitted by the Rietveld method using the TOPAS Academic program suite [42], and is provided as Supplemental Material [43]. Two phases of PbO_2 were identified, a minority α-phase (10.4 wt%, space group $Pbcn$, $a = 5.001$ Å, $b = 5.931$ Å, and $c = 5.443$ Å) and a majority β-phase (89.6 wt%, space group $P42/mnm$, $a = 4.951$ Å, and $c = 3.383$ Å). For β-PbO_2 the oxygen occupancy and oxygen x and y site parameters were refined independently, as were the unit cell lattice parameters and the anisotropic thermal parameters for Pb and O. The peak profiles were modeled with Lorentzian and Gaussian functions and a weighted-profile reliability factor of 1.88% achieved. Analysis of the atomic occupancies confirmed an oxygen deficiency of approximately 1.6%, with an oxygen occupancy of 0.984.

Geometry and Electronic Structure.—PbO_2 (mineral name plattnerite) crystallizes in the rutile structure (β-phase), in which Pb is coordinated to six oxygen in a distorted octahedron (4 short bonds, two long bonds, D_{4h} symmetry) and each oxygen is coordinated to three Pb, via two long bonds and one short bond. The calculated structural and band gap data for PbO_2 are shown in Table I. For comparison we calculated the band structure using both the hybrid HSE06 functional and the semilocal PBE functional. The PBE method overestimates the experimental lattice constants by ~2%, whereas the HSE06 method results in a structure in excellent agreement. The major difference between the PBE and HSE06 electronic structure is that the HSE06 functional predicts PbO_2 to be a semiconductor with a finite band gap, and the PBE predicts a metallic material with an overlap of 0.7 eV of the valence and conduction bands at the Γ point. Analysis of the HSE06 calculated total and partial electronic density of states (PEDOS), Fig. 1(a), shows that the upper valence band is dominated by O $2p$ states, with the lower conduc-

TABLE I. Crystal and electronic structure data for PbO_2 calculated using PBE and HSE06 functionals, and compared to experiment. a and c are the lattice parameters, measured in Å, E_g^{dir} is the direct band gap in eV, E_g^{ind} is the indirect band gap in eV, VB width is the width of the main valence band in eV.

	PBE	HSE06	Experiment
a	5.0602	4.9602	4.9509(2)[a]
c	3.4546	3.3759	3.3830(2)[a]
E_g^{dir}	−0.70	0.35	⋯
E_g^{ind}	⋯	0.23	0.61 [44]
VB width	8.02	8.45	~9.00 [44]
O site occupancy			0.984 (4)[a]

[a]Obtained from refinement of neutron diffraction data of β-PbO_2.

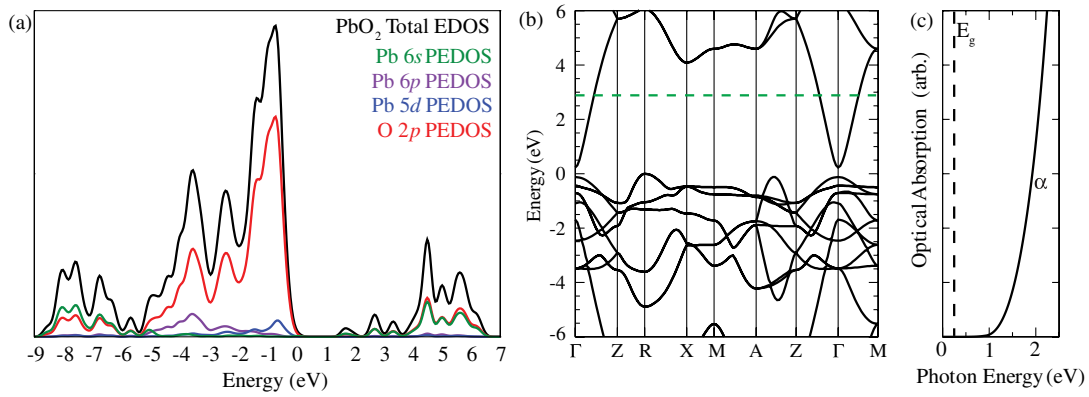

FIG. 1 (color online). HSE06 calculated (a) electronic density of states for PbO_2 with a gaussian smearing of 0.2 eV, (b) band structure for PbO_2, with the position of the calculated charge neutrality level indicated by the horizontal dashed (green) line, and (c) theoretical optical absorption onset of PbO_2.

tion band comprised mostly of Pb 6*s* states. The HSE06 calculated band structure is shown in Fig. 1(b). The VBM is situated at the *R* point, with the conduction band minimum situated at Γ point, resulting in an indirect band gap of 0.23 eV and a direct band gap of 0.35 eV at the Γ point.

To understand the difference between the *fundamental* indirect band gap, and the *optical* band gaps reported in the literature [12,44], we have computed the optical absorption spectra for PbO_2, with the results presented in Fig. 1(c). The onset of optical absorption begins at ~1 eV and increases steadily. The reason for the large difference between the optical band gap and the fundamental band gap can be explained by analyzing the allowed transitions from the valence band to the conduction band. The onset of strong optical absorption does not begin until 0.70 eV below the VBM at Γ, as transitions from above this point are symmetry forbidden. This type of behavior is known for isoelectronic SnO_2 [45,46], and similar behavior has been established for In_2O_3 [47], and Tl_2O_3 [48].

The conduction band of PbO_2 is found to be dispersive around the zone center, with an electron effective mass of $0.18m_e$. The calculated mass is significantly smaller than the value of $0.80m_e$ derived from electrical measurements of a highly degenerate sample [10]. However, given the known values of *ca.* $0.3m_e$ for ZnO, In_2O_3, and SnO_2, which all have much larger band gaps, a smaller value is expected for PbO_2, and therefore electrical transport measurements for PbO_2 should be revisited.

Defective PbO_2.—The formation of charged point defects in a lattice can be compensated by electronic (or ionic [49]) defects. The defects considered in this study include the positively charged V_O and Pb_i, which are electron compensated, as well as the negatively charged oxygen interstitial (O_i) and lead vacancy (V_{Pb}) centers, which are hole compensated. The energy of the electrons and holes are determined by the electron chemical potential (Fermi level).

Figure 2 shows a plot of formation energy for all point defects under O-rich and O-poor regimes. For *n*-type defects, the V_O is the most stable defect under both sets of conditions for high values of the Fermi level, and will be further stabilized at high temperatures by the configurational entropy of O_2, which is neglected in our model but will be partially compensated by the negative vibrational entropy of the vacancy [50]. The Pb_i, which had previously been suggested as the dominant defect [17], is competitive in energy across the span of the band gap, but for highly *n*-type samples, V_O will dominate. V_O exists in the +2 charge state for all chemical potentials: a doubly ionized donor. Our neutron diffraction measurements confirm oxygen substoichiometry at a level of 1.6%, which validates the calculations directly, and is consistent with typical electron carrier concentrations of β-PbO_2.

Based on previous reports of PbO_2 electrodes being lead deficient [14,15,19], one would expect the formation energy of the positively charged defects to be lower than, or equivalent to those of the negatively charged defects. Upon examining Fig. 2, we find that this clearly is not the case. Even under O-rich conditions, the formation energy of 7 eV is so prohibitively high that the concentration of V_{Pb} should be negligible under equilibrium conditions. In SnO_2, a similar conclusion is reached about the concentration of V_{Sn} [20]. The presence of these defects could be explained by defect aggregates formed in the presence of hydroxylated anion sites. Turning to the O_i, we find that it relaxes from the ideal interstitial site towards a lattice oxygen, displacing it to form a peroxide (O-O dumbell-like) species. This type of behavior has also been noted for CdO [51], ZnO [52,53], Al_2O_3 [54], TiO_2 [55,56], and SnO_2 [20,21]. Although the formation energy of O_i is lower than that of V_{Pb}, its ionization levels are deep in the conduction band, indicating that it will not act as an effective charge compensating defect in PbO_2. Under conditions that allow for oxygen exchange with the environment, V_O will be the dominant donor species, and the material will be substoichiometric on the *oxygen* sublattice, with charge compensation occurring through electrons in the conduction band.

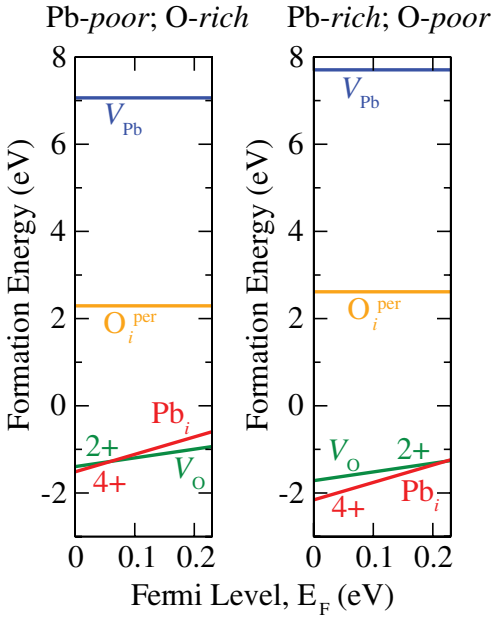

FIG. 2 (color online). Formation energies for intrinsic defects under O-rich conditions (left panel) and O-poor conditions (right panel).

Doping limits.—Typical carrier densities of as-prepared samples of PbO_2 exceed the threshold of the Mott criterion [57,58], such that the material falls into the regime of a degenerate semiconductor, with the Fermi level situated within the conduction band. Taking the critical carrier concentration (n) of $n^{1/3}a_0 > 0.26$, where a_0 is the effective Bohr radius ($\frac{4\pi\epsilon_0\hbar^2}{m^*e^2}$), results in an electron radius of 29 Å and an associated critical carrier concentration of 7×10^{17} cm^{-3}. Once this threshold is exceeded, the material will behave as a metallic conductor and occupation of the conduction band will result in a Moss-Burstein blue-shift in the onset of optical absorption [59].

We can estimate the doping limit (an upper threshold for equilibrium carrier concentration) following the model of the charge neutrality level [60,61]. Utilizing the formalism proposed by Bechstedt and coworkers [62], we find that the charge neutrality level of PbO_2 lies 2.66 eV *above* the conduction band minimum, indicating that this material will be n-type. This is consistent with the calculated defect energies, which indicate that no charge compensation by ionic defects will occur until the Fermi level is more than 2 eV above the conduction band. This yields an approximate *maximum* carrier concentration of 10^{21} cm^{-3}, which is in direct agreement with the reported value [10], as well as the high level of oxygen nonstoichiometric observed in the diffraction measurements. Assuming that oxygen vacancy states are doubly ionized an oxygen deficiency of 1.6% as found by neutron diffraction corresponds to a carrier concentration of 1.5×10^{21} cm^{-3}.

Summary.—We have reported that PbO_2 is semiconducting material with a finite fundamental band gap. Under standard preparative conditions, the material is grossly (1.6%) oxygen deficient, resulting in high electron carrier concentrations. Remarkably, the material can sustain a high donor concentration without self-compensation by negatively charged point defects, which is further validated by a calculated charge neutrality level that is deep in the conduction band.

This work was supported by SFI through the PI program (Grant No. 06/IN.1/I92 and No. 06/IN.1/I92/EC07). Calculations were performed on the TCHPC computing clusters, the Stokes cluster as maintained by ICHEC, and the University of Bath's High Performance Computing Facility. A. W. acknowledges support from the U.K.'s HPC Materials Chemistry Consortium, which is funded by EPSRC Grant No. EP/F067496, and the EPSRC solar fuel Grant No. EP/I01330X.

[1] G. Planté, C.R. Hebd. Seances Acad. Sci. **50**, 640 (1860), http://gallica.bnf.fr/ark:/12148/bpt6k3007r.image.
[2] X. Li, D. Pletcher, and F. C. Walsh, Chem. Soc. Rev. **40**, 3879 (2011).
[3] R. Ahuja, A. Blomqvist, P. Larsson, P. Pyykko, and P. Zaleski-Ejgierd, Phys. Rev. Lett. **106**, 018301 (2011).
[4] L. H. Piette and H. E. Weaver, J. Chem. Phys. **28**, 735 (1958).
[5] D. A. Frey and H. E. Weaver, J. Electrochem. Soc. **107**, 930 (1960).
[6] L. A. Boyarskii, S. P. Gabuda, S. G. Kozlova, and R. N. Pletnev, Low Temp. Phys. **28**, 691 (2002).
[7] D. J. Payne, R. G. Egdell, W. Hao, J. S. Foord, A. Walsh, and G. W. Watson, Chem. Phys. Lett. **411**, 181 (2005).
[8] D. J. Payne, R. G. Egdell, D. S. L. Law, P. A. Glans, T. Learmonth, K. E. Smith, J. H. Guo, A. Walsh, and G. W. Watson, J. Mater. Chem. **17**, 267 (2007).
[9] D. J. Payne *et al.*, Phys. Rev. B **75**, 153102 (2007).
[10] J. P. Pohl and G. L. Schlectriemen, J. Appl. Electrochem. **14**, 521 (1984).
[11] M. Heinemann, H. J. Terpstra, C. Haas, and R. A. Degroot, Phys. Rev. B **52**, 11740 (1995).
[12] W. Mindt, J. Electrochem. Soc. **116**, 1076 (1969).
[13] D. Raviendra, Phys. Rev. B **33**, 2660 (1986).
[14] J. D. Jorgensen, R. Varma, F. J. Rotella, G. Cook, and N. P. Yao, J. Electrochem. Soc. **129**, 1678 (1982).
[15] P. Rüetschi, J. Electrochem. Soc. **139**, 1347 (1992).
[16] P. T. Moseley, J. L. Hutchison, and M. A. M. Bourke, J. Electrochem. Soc. **129**, 876 (1982).
[17] J. P. Carr and N. A. Hampson, Chem. Rev. **72**, 679 (1972).
[18] P. T. Moseley, J. L. Hutchison, C. J. Wright, M. A. M. Bourke, R. I. Hill, and V. S. Rainey, J. Electrochem. Soc. **130**, 829 (1983).
[19] R. J. Hill, Mater. Res. Bull. **17**, 769 (1982).
[20] P. Agoston, C. Korber, A. Klein, M. J. Puska, R. M. Nieminen, and K. Albe, J. Appl. Phys. **108**, 053511 (2010).
[21] K. G. Godinho, A. Walsh, and G. W. Watson, J. Phys. Chem. C **113**, 439 (2009).

[22] G. Kresse and J. Furthmüller, Phys. Rev. B **54**, 11169 (1996).
[23] G. Kresse and D. Joubert, Phys. Rev. B **59**, 1758 (1999).
[24] J. P. Perdew, K. Burke, and M. Ernzerhof, Phys. Rev. Lett. **77**, 3865 (1996).
[25] A. V. Krukau, O. A. Vydrov, A. F. Izmaylov, and G. E. Scuseria, J. Chem. Phys. **125**, 224106 (2006).
[26] J. P. Allen, D. O. Scanlon, and G. W. Watson, Phys. Rev. B **81**, 161103(R) (2010).
[27] B. G. Janesko, T. M. Henderson, and G. E. Scuseria, Phys. Chem. Chem. Phys. **11**, 443 (2009).
[28] D. O. Scanlon and G. W. Watson, J. Phys. Chem. Lett. **1**, 2582 (2010).
[29] J. E. Peralta, J. Heyd, G. E. Scuseria, and R. L. Martin, Phys. Rev. B **74**, 073101 (2006).
[30] D. O. Scanlon, B. J. Morgan, G. W. Watson, and A. Walsh, Phys. Rev. Lett. **103**, 096405 (2009).
[31] D. O. Scalon and G. W. Watson, J. Mater. Chem. **21**, 3655 (2011).
[32] Q. Yan, P. Rinke, M. Winkelnkemper, A. Qteish, D. Bimberg, M. Scheffler, and C. G. Van de Walle, Semicond. Sci. Technol. **26**, 014037 (2011).
[33] F. Tran and P. Blaha, Phys. Rev. B **83**, 235118 (2011).
[34] J. B. Varley, A. Janotti, A. K. Singh, and C. G. Van de Walle, Phys. Rev. B **79**, 245206 (2009).
[35] F. Oba, A. Togo, I. Tanaka, J. Paier, and G. Kresse, Phys. Rev. B **77**, 245202 (2008).
[36] M. Gajdos, K. Hummer, G. Kresse, J. Furthmuller, and F. Bechstedt, Phys. Rev. B **73**, 045112 (2006).
[37] C. G. Van de Walle and J. Neugebauer, J. Appl. Phys. **95**, 3851 (2004).
[38] S. B. Zhang and J. E. Northrup, Phys. Rev. Lett. **67**, 2339 (1991).
[39] C. Freysoldt, J. Neugebauer, and C. G. Van de Walle, Phys. Rev. Lett. **102**, 016402 (2009).
[40] S. Lany and A. Zunger, Phys. Rev. B **78**, 235104 (2008).
[41] S. Hull, R. I. Smith, W. I. F. David, A. C. Hannon, J. Mayers, and R. Cywinski, Physica B (Amsterdam) **180-181**, 1000 (1992).
[42] A. A. Coelho, *TOPAS: General Profile and Structure Analysis Software for Powder Diffraction Data, 4.1: Bruker AXS:* (Karlsruhe, Germany, 2007).
[43] See Supplemental Material at http://link.aps.org/supplemental/10.1103/PhysRevLett.107.246402 for the observed and calculated neutron diffraction data.
[44] D. J. Payne, G. Paolicelli, F. Offi, G. Panaccione, P. Lacovig, G. Beamson, A. Fondacaro, G. Monaco, G. Vanko, and R. G. Egdell, J. Electron Spectrosc. Relat. Phenom. **169**, 26 (2009).
[45] A. Schleife, J. B. Varley, F. Fuchs, C. Rödl, F. Bechstedt, P. Rinke, A. Janotti, and C. G. Van de Walle, Phys. Rev. B **83**, 035116 (2011).
[46] J. Robertson, J. Phys. C **12**, 4767 (1979).
[47] A. Walsh, J. L. F. Da Silva, S. H. Wei, C. Korber, A. Klein, L. F. J. Piper, A. DeMasi, K. E. Smith, G. Panaccione, and P. Torelli *et al.*, Phys. Rev. Lett. **100**, 167402 (2008).
[48] A. B. Kehoe, D. O. Scanlon, and G. W. Watson, Phys. Rev. B **83**, 233202 (2011).
[49] C. R. A. Catlow, A. A. Sokol, and A. Walsh, Chem. Commun. (Cambridge) **47**, 3386 (2011).
[50] A. Walsh, A. A. Sokol, and C. R. A. Catlow, Phys. Rev. B **83**, 224105 (2011).
[51] M. Burbano, D. O. Scanlon, and G. W. Watson, J. Am. Chem. Soc. **133**, 15065 (2011).
[52] A. Janotti and C. G. Van de Walle, Phys. Rev. B **76**, 165202 (2007).
[53] A. A. Sokol, S. A. French, S. T. Bromley, C. R. A. Catlow, H. J. J. van Dam, and P. Sherwood, Faraday Discuss. **134**, 267 (2007).
[54] A. A. Sokol, A. Walsh, and C. R. A. Catlow, Chem. Phys. Lett. **492**, 44 (2010).
[55] B. J. Morgan and G. W. Watson, Phys. Rev. B **80**, 233102 (2009).
[56] S. Na-Phattalung, M. F. Smith, K. Kim, M.-H. Du, S.-H. Wei, S. B. Zhang, and S. Limpijumnong, Phys. Rev. B **73**, 125205 (2006).
[57] N. F. Mott, Rev. Mod. Phys. **40**, 677 (1968).
[58] P. P. Edwards and M. J. Sienko, Phys. Rev. B **17**, 2575 (1978).
[59] P. P. Edwards, A. Porch, M. O. Jones, D. V. Morgan, and R. M. Perks, Dalton Trans. 2995 (2004).
[60] J. Tersoff, Phys. Rev. B **30**, 4874 (1984).
[61] J. Robertson and B. Falabretti, J. Appl. Phys. **100**, 014111 (2006).
[62] A. Schleife, F. Fuchs, C. Rödl, J. Furthmüller, and F. Bechstedt, Appl. Phys. Lett. **94**, 012104 (2009).